VI International Conference on Computational Methods for Coupled Problems in Science and Engineering
COUPLED PROBLEMS 2015
B. Schrefler, E. Oñate and M. Papadrakakis (Eds)

BOUNDARY ELEMENT SOLUTION OF 2D COUPLED PROBLEM IN ANISOTROPIC PIEZOELECTRIC FGM PLATES

MOHAMED ABDELSABOUR FAHMY*, †

[*] Jummum University College
Umm Al-Qura University
Alazizya, behind Alsalam Souq, 21955 Makkah, Saudi Arabia.
e-mail: maselim@uqu.edu.sa, Web page: https://uqu.edu.sa/staff/ar/4340548

[†] Faculty of Computers and Informatics
Suez Canal University
Old Campus, El-Sheikh Zayed, 41522 Ismailia, Egypt.
e-mail: Mohamed_fahmy@ci.suez.edu.eg
Web page: http://mohamed_fahmy_ci.staff.scuegypt.edu.eg

Key words: Plate; Piezoelectric; Stress; Anisotropic; functionally graded material; Dual reciprocity boundary element method.

Abstract. The mechanics of the piezoelectric functionally graded material (FGM) has received considerable research effort with their increasing usage in various applications including sensors and actuators, piezoelectric motors, reduction of vibrations and noise, infertility treatment and photovoltaics. It is hard to find the analytical solution of a problem in a general case, therefore, an important number of engineering and mathematical papers devoted to the numerical solution have studied the overall behavior of such materials. The time-stepping dual reciprocity boundary element method was proposed to solve the 2D coupled problem in anisotropic piezoelectric FGM plates. The accuracy of the proposed method was examined and confirmed by comparing the obtained results with those known previously.

1 INTRODUCTION

Numerical modelling of piezoelectric solids present certain difficulties since they exhibit not only electro-elastic coupling but anisotropic behaviour. Piezoelectric effect can only appear in crystals that lack of a centre of symmetry and that, as a consequence, are anisotropic. This anisotropy reduces in most cases to transversal isotropy. Piezoelectric ceramics are used for construction of sensors, transducers, actuators as well as adaptative structures. Lead zirconate titanate (PZT) is the most widely used piezoceramic. There are also piezopolymers as the polyvinilidene fluoride (PVDF). Owing to the coupling effects between mechanical and electric properties, piezoelectric materials (PMs) have found wide technological applications as sensors and actuators, piezoelectric motors, reduction of vibrations and noise, infertility treatment and photovoltaics. Applications of piezoelectric materials as electro-mechanical devices have also stimulated a wide range of analytical researches [1-14]. It is usually difficult to obtain analytical solutions to problems involving finite solids or complex boundary conditions. Numerical methods, such as the finite difference method [15-19], the finite element method [20] and the boundary element method (BEM) [21-31] have also been applied to the analysis of electromechanical coupling under complicated conditions. Pan [32] derived the Green's functions for the anisotropic piezoelectric solids in an infinite plane, a half plane, and two joined dissimilar half-planes using the complex variable function method and presented a single-domain BEM analysis of 2D facture mechanics. Recent developments of 2D Green's functions and BEM analysis can be found in Refs. [33–37] for example. It is well known that the BEM presents significant advantages over other numerical techniques for the analysis of fracture mechanics problems. This fact has led to the publication of several BE approaches for the analysis of cracks in piezoelectric solids in the last few years. Presence of domain integrals in the formulation of the BEM dramatically decreases the efficiency of this technique. One of the most frequently used techniques for converting the domain integral into a boundary one developed through our paper is the so-called dual reciprocity boundary element method (DRBEM) [38-46].

In this article the DRBEM is used to solve the coupled problem in anisotropic piezoelectric FGM plates. In the case of two-dimensional, a numerical scheme for the implementation of the method is presented. The accuracy of the proposed method was examined and confirmed by comparing the obtained results with those known before.

2 FORMULATION OF THE PROBLEM

Here, we present the basic equations of the piezoelectric elasticity theory, which will be used for the solution of the problem described in the Introduction. With reference to a Cartesian coordinate system (x, y, z) as shown in Fig. 1. We shall consider a functionally graded anisotropic piezoelectric plate. The plate occupies the region $R = \{(x, y, z): 0 < x < \zeta, 0 < y < \Psi, 0 < z < \xi$ with graded material properties in the thickness direction.

In this paper, the FGM properties are graded along the thickness direction (x-direction) of the plate. The governing equations for the stress wave propagation in anisotropic functionally graded piezoelectric plate may be written in the following form

$$C_{fghi}u_{h,if} = \rho\ddot{u}_g - C_{fghi}\aleph u_{h,i} - e_{ifg}\left\lfloor \Phi_{,if} + \aleph\Phi_{,i} \right\rfloor \tag{1}$$

$$e_{fhi}u_{h,if} = \epsilon_{fi}\Phi_{,if} - e_{fhi}\aleph u_{h,i} + \epsilon_{fi}\left[\Phi_{,if} + \aleph\Phi_{,i}\right] \tag{2}$$

where σ_{fg} is the mechanical stress tensor, ε_{hi} is the strain tensor, u_h is the displacement vector, E_i is the electric field vector, Φ is the electric potential, D is the electric displacement, C_{fghi} is the elasticity tensor $\left(C_{fghi} = C_{gfhi} = C_{hifg}\right)$, e_{ifg} is the piezoelectric tensor $\left(e_{ifg} = eigf, \epsilon fi\right.$ is the permittivity tensor $\epsilon fi = \epsilon if$, ρ is the density and $\aleph = mx+1$.

A superposed dot denotes differentiation with respect to the time and a comma followed by a subscript denotes partial differentiation with respect to the corresponding coordinates.

3 NUMERICAL IMPLEMENTATION

Using the contracted notation, the governing equations (1) and (2) can be combined to form a single equation as follows:

$$L_{\mathrm{GH}} U_{\mathrm{H}} = \rho \delta_{GH} \ddot{U}_{\mathrm{H}} - \mathrm{B}_{\mathrm{G}} \tag{3}$$

where

$$U_{\mathrm{H}} = \begin{cases} u_h & h = \mathrm{H} = 1,2,3 \\ \Phi & \mathrm{H} = 4 \end{cases} \tag{4}$$

$$\mathrm{Z}_{\mathrm{G}} = \begin{cases} t_g & g = G = 1,2,3 \\ q & G = 4 \end{cases} \tag{5}$$

$$C_{f\mathrm{GH}i} = \begin{cases} C_{fghi}, & g = \mathrm{G} = 1,2,3; h = \mathrm{H} = 1,2,3 \\ \mathrm{e}_{ifg}, & g = \mathrm{G} = 1,2,3; \mathrm{H} = 4 \\ \mathrm{e}_{fhi}, & \mathrm{G} = 4; \quad h = \mathrm{H} = 1,2,3 \\ -\epsilon_{fi}, & \mathrm{G} = 4; \quad \mathrm{H} = 4 \end{cases} \tag{6}$$

$$\delta_{GH} = \begin{cases} \delta_{gh} & g = G = 1,2,3, \quad k = K = 1,2,3 \\ 0 & otherwise \end{cases} \tag{7}$$

$$L_{\mathrm{GH}} = C_{f\mathrm{GH}i} \frac{\partial}{x_i} \frac{\partial}{x_f} \tag{8}$$

$$\mathrm{B}_{\mathrm{G}} = \begin{cases} C_{fghi} \bar{\bar{u}} + \mathrm{e}_{ifg} \bar{\bar{\Phi}}, & g = G = 1,2,3 \\ \epsilon_{fi} \Phi_{,if} - \mathrm{e}_{fhi} \bar{\bar{u}} + \epsilon_{fi} \bar{\bar{\Phi}}, & G = 4 \end{cases} \tag{9}$$

$$\bar{\bar{u}} = \aleph u_{h,\mathrm{i}}, \qquad \bar{\bar{\Phi}} = \Phi_{,if} + \aleph \Phi_{,i} \tag{10}$$

Now, we choose the fundamental solution U_{MH}^{*} as weighting function as follows

$$L_{GH} U_{MH}^{*}(x,\xi) = -\delta_{GM} \delta(x,\xi) \tag{11}$$

By integrating the weighted residual formula by parts twice we obtain the following piezoelectric reciprocity relation

$$\int_R \left(L_{\mathrm{GH}} \mathrm{U}_H U_{MG}^{*} - L_{\mathrm{GH}} U_{MH}^{*} \mathrm{U}_{\mathrm{G}} \right) dR = \int_\Gamma \left(U_{MG}^{*} \mathrm{Z}_{\mathrm{G}} - \mathrm{Z}_{MG}^{*} \mathrm{U}_{\mathrm{G}} \right) d\Gamma \tag{12}$$

where

$$\mathrm{Z}_{MG}^{*} = C_{f\mathrm{G}Hi} U_{MH,i}^{*} n_f$$

By the use of sifting property, we obtain from equation (12) the piezoelectric integral representation formula

$$U_{\mathrm{M}}(\xi) = \int_\Gamma \left(U_{MG}^{*} \mathrm{Z}_{\mathrm{G}} - \mathrm{Z}_{MG}^{*} \mathrm{U}_{\mathrm{G}} \right) d\Gamma - \int_R U_{MG}^{*} \left(\rho \delta_{GH} \ddot{U}_{\mathrm{H}} - \mathrm{B}_{\mathrm{G}} \right) dR \tag{13}$$

To transform the domain integrals into boundary integrals over the global boundary of the analyzed domain, the DRBEM can be applied to equation (13) to give the dual reciprocity representation formula of piezoelectric as

$$U_H(\xi) = \int_\Gamma \left(U_{HG}^{*} \mathrm{Z}_{\mathrm{G}} - \mathrm{Z}_{HG}^{*} \mathrm{U}_{\mathrm{G}} \right) d\Gamma + \sum_{q=1}^{N} \left(U_{HN}^{q}(\xi) + \int_\Gamma \left(T_{HG}^{*} U_{GN}^{q} - \mathrm{U}_{HG}^{*} T_{GN}^{q} \right) d\Gamma \right) \alpha_{\mathrm{N}}^{\mathrm{q}} \tag{14}$$

According to the steps described in Fahmy [43], the dual reciprocity boundary integral equation (14) can be written in the following system of equations

$$\bar{\zeta}\breve{U}(t) - \bar{\eta}\breve{T}(t) = \left(\bar{\zeta}\breve{\mho}(t) - \bar{\eta}\breve{\tau}(t)\right)\alpha(t) \tag{15}$$

where $\bar{\zeta}$, $\bar{\eta}$ are BEM system matrices, $\breve{U}$, $\breve{T}$ contain the nodal values of the generalized displacements and fluxes, and $\breve{\mho}$, $\breve{\tau}$ contain the particular solutions

The coefficient vector $\alpha_s(t)$ can be calculated by setting up a system of N equations from (15) using the point collocation procedure, which yields the system

$$M\ddot{\breve{U}}(t) + \bar{\zeta}\breve{U}(t) = \bar{\eta}\breve{T}(t) + \breve{\mathcal{B}}(t) \tag{16}$$

where the volume matrix V, piezoelectric mass matrix M and source vector $\breve{\mathcal{B}}(t)$ are as follows:

$$V = \left(\bar{\eta}\breve{\tau}(t) - \bar{\zeta}\breve{\mho}(t)\right)\mathcal{F}^{-1}, \qquad M = \rho V, \quad \breve{\mathcal{B}}(t) = V\breve{B}(t). \tag{17}$$

The following matrix equation is obtained from Eq. (16).

$$\begin{bmatrix} M^{11} & M^{12} \\ M^{21} & M^{22} \end{bmatrix}\begin{bmatrix} \ddot{U}^{k} \\ \ddot{U}^{u} \end{bmatrix} + \begin{bmatrix} K^{11} & K^{12} \\ K^{21} & K^{22} \end{bmatrix}\begin{bmatrix} U^{k}(t) \\ U^{u}(t) \end{bmatrix} = \begin{bmatrix} \bar{\eta}^{11} & \bar{\eta}^{12} \\ \bar{\eta}^{21} & \bar{\eta}^{22} \end{bmatrix}\begin{bmatrix} T^{k}(t) \\ T^{u}(t) \end{bmatrix} + \begin{bmatrix} \mathcal{B}^{1}(t) \\ \mathcal{B}^{2}(t) \end{bmatrix} \tag{18}$$

The unknown fluxes $T^{u}(t)$ are obtained from the first row of matrix equation (18) and are expressed as follows.

$$\begin{aligned} T^{u}(t) = (\eta^{12})^{-1}\big[& M^{11}\ddot{U}^{k}(t) + M^{12}\ddot{U}^{u}(t) + K^{11}U^{k}(t) \\ & + K^{11}U^{k}(t) + K^{12}U^{u}(t) - \bar{\eta}^{11}T^{k}(t) - \mathcal{B}^{1}(t)\big] \end{aligned} \tag{19}$$

Making use of Eq. (19), we can write the second row of matrix equation (18) as

$$M^{u}\ddot{U}^{u}(t) + K^{u}U^{u}(t) = Q^{k}(t) \tag{20}$$

where

$$Q^{k}(t) = \bar{\mathcal{B}}^{k}(t) + \bar{\eta}^{k}T^{k}(t) - M^{k}\ddot{U}^{k}(t) - K^{k}U^{k}(t)$$
$$M^{u} = M^{22} - \bar{\eta}^{22}(\bar{\eta}^{12})^{-1}M^{12}$$
$$M^{k} = M^{21} - \bar{\eta}^{22}(\bar{\eta}^{12})^{-1}M^{11}$$
$$K^{u} = K^{22} - \bar{\eta}^{22}(\bar{\eta}^{12})^{-1}K^{12}$$
$$K^{k} = K^{21} - \bar{\eta}^{22}(\bar{\eta}^{12})^{-1}K^{11}$$
$$\bar{\eta}^{k} = \bar{\eta}^{21} - \bar{\eta}^{22}(\bar{\eta}^{12})^{-1}\eta^{11}$$
$$\bar{\mathcal{B}}^{k}(t) = \mathcal{B}^{2}(t) - \bar{\eta}^{22}(\bar{\eta}^{12})^{-1}\mathcal{B}^{1}(t)$$

We now split the system (20) into elastic and electric parts as follows:

$$\begin{bmatrix} M^{u}_{uu} & 0 \\ M^{u}_{\varphi u} & 0 \end{bmatrix}\begin{bmatrix} \ddot{u}^{u}(t) \\ \ddot{\varphi}^{u}(t) \end{bmatrix} + \begin{bmatrix} K^{u}_{uu} & K^{u}_{u\varphi} \\ K^{u}_{\varphi u} & K^{u}_{\varphi\varphi} \end{bmatrix}\begin{bmatrix} u^{u}(t) \\ \varphi^{u}(t) \end{bmatrix} = \begin{bmatrix} Q^{k}_{u}(t) \\ Q^{k}_{\varphi}(t) \end{bmatrix} \tag{21}$$

The unknown electric potential φ^{u} can be obtained from the second row of Eq. (21) as

$$\varphi^{u}(t) = \left(K^{u}_{\varphi\varphi}\right)^{-1}\left[Q^{k}_{\varphi}(t) - M^{u}_{\varphi u}\ddot{u}^{u}(t) - K^{u}_{\varphi u}u^{u}(t)\right] \tag{22}$$

With the aid of Eq. (22) into the first row of Eq. (21) we obtain

$$\bar{M}^{u}\ddot{u}^{u}(t) + \bar{K}^{u}u^{u}(t) = \bar{Q}^{k}(t) \tag{23}$$

where

$$\bar{Q}^{k}(t) = Q^{k}_{u}(t) - K^{u}_{u\varphi}\left(K^{u}_{\varphi\varphi}\right)^{-1}Q^{k}_{\varphi}(t)$$
$$\bar{M}^{u} = M^{u}_{uu} - K^{u}_{u\varphi}\left(K^{u}_{\varphi\varphi}\right)^{-1}M^{u}_{\varphi u}$$
$$\bar{K}^{u} = K^{u}_{uu} - K^{u}_{u\varphi}\left(K^{u}_{\varphi\varphi}\right)^{-1}K^{u}_{\varphi u}$$

We can write Eq. (23) at time step $n+1$

$$\bar{M}^u \ddot{u}^u_{\mathrm{n+1}} + \bar{K}^u u^u_{\mathrm{n+1}} = \bar{Q}^{\mathrm{k}}_{\mathrm{n+1}} \tag{24}$$

where

$$\bar{Q}^{\mathrm{k}}_{\mathrm{n+1}} = \bar{\mathcal{B}}^{\mathrm{k}}_{\mathrm{n+1}} + \eta^{\mathrm{k}} \mathrm{T}^{\mathrm{k}}_{\mathrm{n+1}} - M^k \ddot{u}^{\mathrm{k}}_{\mathrm{n+1}} - K^k u^{\mathrm{k}}_{\mathrm{n+1}} \tag{25}$$

The displacements u_{n+1} and velocities $\dot{u}_{\mathrm{n+1}}$ used in this algorithm are approximated at time step n+1 as follows:

$$\dot{u}_{\mathrm{n+1}} \approx \dot{u}_{\mathrm{n}} + [(1-\delta)\ddot{u}_{\mathrm{n}} + \delta \ddot{u}_{\mathrm{n+1}}]\Delta \mathrm{t} \tag{26}$$

$$u_{n+1} \approx u_n + \dot{u}_{\mathrm{n}} \Delta \mathrm{t} + \left[\left(\frac{1}{2} - \alpha\right)\ddot{u}_{\mathrm{n}} + \alpha \ddot{u}_{\mathrm{n+1}}\right]\Delta \mathrm{t}^2 \tag{27}$$

The acceleration at time step n+1 may be expressed from Equation (27) as:

$$\ddot{u}_{\mathrm{n+1}} \approx \frac{1}{\alpha \Delta \mathrm{t}^2}(u_{n+1} - u_n) - \frac{1}{\alpha \Delta \mathrm{t}} \dot{u}_{\mathrm{n}} - \left(\frac{1}{2\alpha} - 1\right)\ddot{u}_{\mathrm{n}} \tag{28}$$

Upon substitution of (28) into (24) we obtain the following algebraic system

$$\mathbb{R} u^{\mathrm{u}}_{\mathrm{n+1}} = \mathcal{M}_{\mathrm{n+1}} \tag{29}$$

where the stiffness matrix $\mathbb{R}$ and effective load vector $\mathcal{M}_{\mathrm{n+1}}$ are given by

$$\mathbb{R} = \frac{1}{\alpha \Delta \mathrm{t}^2} \bar{M}^u + \bar{K}^u \tag{30}$$

$$\mathcal{M}_{\mathrm{n+1}} = \bar{Q}^{\mathrm{k}}_{\mathrm{n+1}} + \bar{M}^u \left[\frac{1}{\alpha \Delta \mathrm{t}^2} u^u_n + \frac{1}{\alpha \Delta \mathrm{t}} \dot{u}^u_n + \left(\frac{1}{2\alpha} - 1\right)\ddot{u}^u_n\right] \tag{31}$$

Once we have solved (29) for the unknown displacements at time step n+1, we can compute the accelerations and velocities from equations (28) and (26) respectively. Finally, the electric potential $\varphi^{\mathrm{u}}(t)$ can be obtained from (22) and the unknown generalized tractions $\mathrm{T}^u(\mathrm{t})$ can be determined using equation (19).

4 NUMERICAL RESULTS AND DISCUSSION

With the view of illustrating the numerical results, the material chosen for the plate is the piezoelectric ceramic Lead Zirconate Titanate (PZT), and the physical data for which is given as follows:

The elasticity tensor C_{fghi}, piezoelectric tensor e and relative permittivity ϵ^{rel}

$$C_{fghi} = \begin{pmatrix} 107.6 & 63.10 & 63.90 & 0.000 & 0.000 & 0.000 \\ 63.10 & 107.6 & 63.90 & 0.000 & 0.000 & 0.000 \\ 63.90 & 63.90 & 100.4 & 0.000 & 0.000 & 0.000 \\ 0.000 & 0.000 & 0.000 & 19.60 & 0.000 & 0.000 \\ 0.000 & 0.000 & 0.000 & 0.000 & 19.60 & 0.000 \\ 0.000 & 0.000 & 0.000 & 0.000 & 0.000 & 22.20 \end{pmatrix}$$

$$e = \begin{pmatrix} 0.00 & 0.00 & 0.00 & 0.00 & 12.0 & 0.00 \\ 0.00 & 0.00 & 0.00 & 12.0 & 0.00 & 0.00 \\ -9.6 & -9.6 & 15.1 & 0.00 & 0.00 & 0.00 \end{pmatrix}$$

$$\epsilon^{\mathrm{rel}} = \begin{pmatrix} 1936 & 0.00 & 0.00 \\ 0.00 & 1936 & 0.00 \\ 0.00 & 0.00 & 2109 \end{pmatrix}$$

the results are plotted in Figs. 2–4 to show the validity of the DRBEM. These results obtained with the DRBEM have been compared graphically with those obtained using the Meshless Local Petrov–Galerkin (MLPG) method of Sladek et al. [47] are shown graphically in the same figures to confirm the validity of the proposed method. It can be seen from these figures that the DRBEM results are in excellent agreement with the results obtained by MLPG. The effects of the number of elements used were also examined. It was found that a further increase of boundary elements in the DRBEM led to improved numerical results (see Figures 2, 3 and 4).

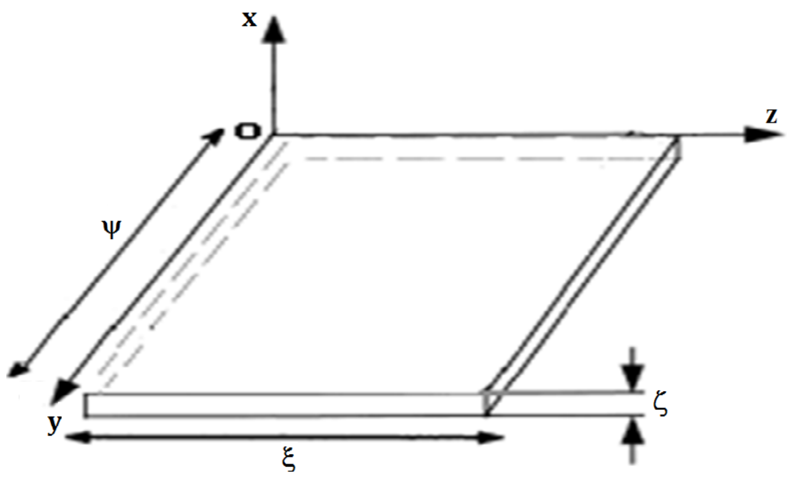

Fig. 1. The coordinate system of the plate.

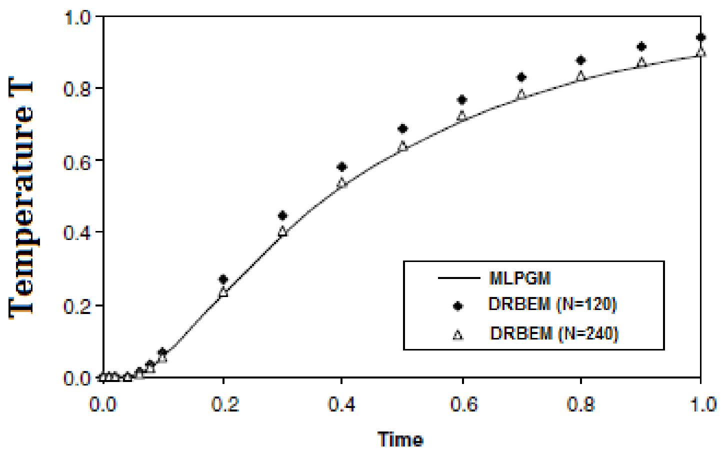

Fig. 2. Variation of the temperature T with time t for MLPGM and DRBEM

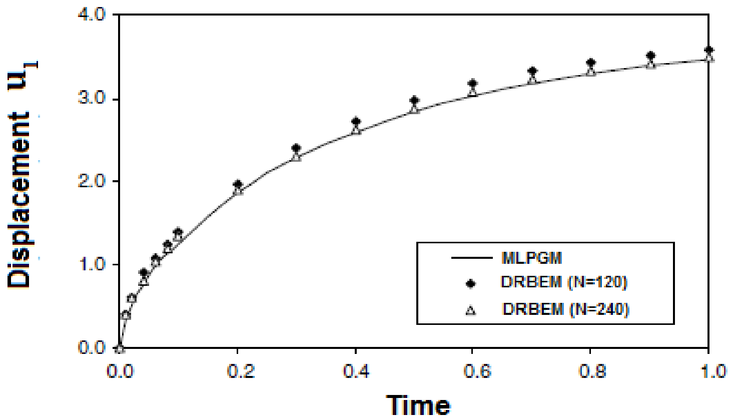

Fig. 3. Variation of the displacement u_1 with time t for MLPGM and DRBEM

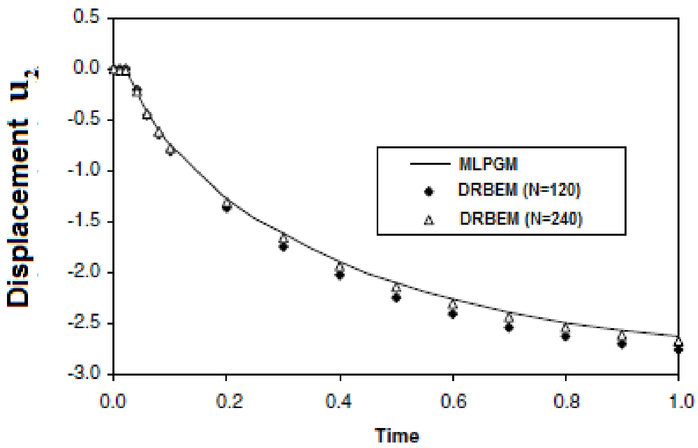

Fig. 4. Variation of the displacement u_2 with time t for MLPGM and DRBEM

REFERENCES

[1] Suo Z, Kuo CM, Barnett DM, Willis JR. Fracture mechanics for piezoelectric ceramics. Journal of the Mechanics and Physics of Solids 1992;40:739–765.
[2] Zhang N, Gao CF. Effects of electrical breakdown on a conducting crack or electrode in electrostrictive solids. European Journal of Mechanics-A/Solids 2012;32:62–68.
[3] Chen YH, Lu TJ. Cracks and fracture in piezoelectric materials. Advances in Applied Mechanics 2002;39:121–215.
[4] Abd-Alla, A.N., Alsheikh, F.A., Reflection and refraction of plane quasi-longitudinal waves at an interface of two piezoelectric media under initial stresses, Archive of Applied Mechanics 79, pp.843–857. (2009).
[5] Abd-Alla, A.N., Al-sheikh, F., Al-Hossain, A.Y., Effect of initial stresses on dispersion relation of transverse waves in a piezoelectric layered cylinder Materials Science and Engineering B: Solid-State Materials for Advanced Technology 162 pp.147–154, (2009).
[6] Abd-Alla, A.N.,Al-sheikh, F., The effect of the initial stresses on the reflection and transmission of plane quasi-vertical transverse waves in piezoelectric materials, World Academy of Science, Engineering and Technology, 50, pp.660-668 (2009).
[7] Suo Z, Kuo CM, Barnett DM, Willis JR. Fracture mechanics for piezoelectric ceramics. J Mech Phys Solids 1992:40:739–65.
[8] Pan EA. BEM analysis of fracture mechanics in 2D anisotropic piezoelectric solids. Eng Anal Bound Elem1999:23:67–76.
[9] Zhang TY, Zhao MH, Tong P. Fracture of piezoelectric ceramics. Adv Appl Mech 2002:38:147–289.
[10] Jin B, Zhong Z. A moving mode-III crack in functionally graded piezoelectric material: permeable problem. Mech Res Commun 2002:29:217–224.
[11] Lin S, Narita F, Shindo Y. Electroelastic analysis of a penny-shaped crack in a piezoelectric ceramic under mode I loading. Mech Res Commun 2003:30: 371–86.
[12] Fang DN, Wan YP, Soh AK. Magnetoelastic fracture of soft ferromagnetic materials. Theor Appl Fract Mech 2004:42:317–34.
[13] Kuna M. Fracture mechanics of piezoelectric materials – where are we right now? Eng Fract Mech 2010:77:309–26.
[14] Zhong XC, Zhang KS. Electroelastic analysis of an electrically dielectric Griffith crack in a piezoelectric layer. Int J Eng Sci 2010:48:612–23.
[15] Abd-Alla AM, El-Naggar AM and Fahmy MA, Magneto-thermoelastic problem in non-homogeneous isotropic cylinder, Heat and Mass Transfer, 2003:39:625-629.
[16] El-Naggar AM, Abd-Alla AM and Fahmy MA, The propagation of thermal stresses in an infinite elastic slab, Applied Mathematics and Computation, 2003:12:220-226.
[17] El-Naggar AM, Abd-Alla AM, Fahmy MA and Ahmed SM, Thermal Stresses in a rotating non-homogeneous orthotropic hollow cylinder, Heat and Mass Transfer, 2002:39:41-46.
[18] Fahmy MA, Thermal stresses in a spherical shell under three thermoelastic models using FDM, International Journal of Numerical methods and Applications, 2009:2:123-128.
[19] Fahmy MA, Finite difference algorithm for transient magneto-thermo-elastic stresses in a non-homogeneous solid cylinder, International Journal of Materials Engineering and Technology, 2010:3:87-93.

[20] Ha SK, Keilers C, Chang FK. Finite element analysis of composite structures containing distributed piezoceramic sensors and actuators. AIAA Journal 1992;30:772–780.

[21] Lee JS. Boundary element method for electroelastic interaction in piezoceramics. Eng Anal Bound Elements 1995;15:321–328.

[22] Abd-Alla AM, El-Shahat TM and Fahmy MA, Thermal stresses in a rotating non-homogeneous anisotropic elastic multilayered solids, Far East Journal of Applied Mathematics 2007:27: 223-243.

[23] Abd-Alla AM, El-Shahat TM and Fahmy MA, Effect of inhomogeneity on the thermoelastic stresses in micro-engineering anisotropic solid, Far East Journal of Applied Mathematics 2007:27:245-264.

[24] Abd-Alla AM, El-Shahat TM and Fahmy MA, Thermoelastic stresses in inhomogeneous anisotropic solid in the presence of body force, International Journal of Heat & Technology 2007:25:111-118.

[25] Abd-Alla AM, Fahmy MA and El-Shahat TM, Magneto-thermo-elastic stresses in inhomogeneous anisotropic solid in the presence of body force, Far East Journal of Applied Mathematics, 2007:27:499-516.

[26] Abd-Alla AM, Fahmy MA and El-Shahat TM, Transient piezothermoelastic stresses in a rotating non-homogeneous composite structure, Far East Journal of Applied Mathematics, 2007:27:489-497.

[27] Fahmy MA, Effect of initial stress and inhomogeneity on magneto-thermo-elastic stresses in a rotating anisotropic solid, JP Journal of Heat and Mass Transfer, 2007:1:93-112.

[28] Abd-Alla AM, Fahmy MA and El-Shahat TM, Magneto-thermo-elastic problem of a rotating non-homogeneous anisotropic solid cylinder, Archive of Applied Mechanics 2008:78:135-148.

[29] Fahmy MA, Thermoelastic stresses in a rotating non- homogeneous anisotropic body, Numerical Heat Transfer, Part A: Applications, 2008:53:1001-1011.

[30] Fahmy MA and El-Shahat TM, The effect of initial stress and inhomogeneity on the thermoelastic stresses in a rotating anisotropic solid, Archive of Applied Mechanics, 2008:78:431-442.

[31] Fahmy MA and Salama SA (2010), Boundary element solution of steady-state temperature distribution in non-homogeneous media, Far East Journal of Applied Mathematics 2010:43:31-40.

[32] Pan EN. A BEM analysis of fracture mechanics in 2D anisotropic piezoelectric solids. Engng Anal Bound Elem 1999;23:67–76.

[33] Denda M, Lua J. Development of the boundary element method for 2D piezoelectricity. Compos, Part B-Engng 1999;30:699–707.

[34] Qin QH, Meng L. BEM for crack-inclusion problems of plane thermopiezoelectric solids. Int J Numeric Meth Engng 2000;48:1071–1088.

[35] Qin QH. Thermoelectroelastic analysis of cracks in piezoelectric halfplane by BEM. Comput Mech 1999;23:353–360.

[36] Gao CF, Wang MZ. Green's functions of an interfacial crack between two dissimilar piezoelectric media. Int J Solids Struct 2001;38: 5323–5334.

[37] Liu Y, Fan H. Analysis of thin piezoelectric solids by the boundary element method. Comput Methods Appl Mech Engng 2002;191:2297–2315.

[38] Fahmy MA, Application of DRBEM to non steady-state heat conduction in non-homogeneous anisotropic media under various boundary elements, Far East Journal of Mathematical Sciences, 2010:43:83-93.
[39] Fahmy MA, Transient magneto-thermoviscoelastic plane waves in a non-homogeneous anisotropic thick strip subjected to a moving heat source, Applied Mathematical Modelling, 2012:36:4565-4578.
[40] Fahmy MA, The effect of rotation and inhomogeneity on the transient magneto-thermoviscoelastic stresses in an anisotropic solid, ASME Journal of Applied Mechanics, 2012:79:1015.
[41] Fahmy MA, Transient magneto-thermo-viscoelastic stresses in a rotating nonhomogeneous anisotropic solid with and without a moving heat source, Journal of Engineering Physics and Thermophysics 2012:85:950-958.
[42] Fahmy MA, Transient magneto-thermo-elastic stresses in an anisotropic viscoelastic solid with and without moving heat source, Numerical Heat Transfer, Part A: Applications 2012:61:547-564.
[43] Fahmy MA, Implicit-Explicit time integration DRBEM for generalized magneto-thermoelasticity problems of rotating anisotropic viscoelastic functionally graded solids, Engineering Analysis with Boundary Elements 2013:37:107-115.
[44] Fahmy MA, Generalized magneto-thermo-viscoelastic problems of rotating functionally graded anisotropic plates by the dual reciprocity boundary element method, Journal of Thermal Stresses 2013:36:1-20.
[45] Fahmy MA, A three-dimensional generalized magneto-thermo-viscoelastic problem of a rotating functionally graded anisotropic solids with and without energy dissipation, Numerical Heat Transfer, Part A: Applications 2013:63:713-733.
[46] Fahmy MA, A Computerized DRBEM model for generalized magneto-thermo-visco-elastic stress waves in functionally graded anisotropic thin film/substrate structures, Latin American Journal of Solids and Structures 2014:11:386-409.
[47] J. Sladek, V. Sladek, P. Stanak, C. Zhang, M. Wünsche, Analysis of the bending of circular piezoelectric plates with functionally graded material properties by a MLPG method, Engineering Structures 2013:47:81–89.